International Journal of Scientific Research & Engineering Trends
Volume 11, Issue 5, Sep-Oct-2025, ISSN (Online): 2395-566X

Synthesis and Characterization of Zinc Oxide Nanowire: Applying Findings to Predict its Uses

Umudi E.Q[1], Ekpenyong I.O[2], Sani M.I[3], Onwugbuta G C[4], Ikechukwu S.C[5], Obruche E.K[6]
[1]Department of Chemical Science, University of Delta, Agbor, Nigeria
[2]Department of Chemical Science, Akwa Ibom State Polytechnic, Ikot Osurua, Ikot Ekpene
[3]Department of Chemistry, Federal University of Education, Zaria, Kaduna State, Nigeria
[4]Department of Biochemistry/Chemistry Technology, University of Port Harcourt, River State
[5]Department of SLT, Imo State Polytechnic, Omuma
[6]Department of Chemistry, Delta State College of Education

Abstract- Zinc Oxide (ZnO) nanowires featuring a hexagonal configuration were successfully synthesized through the chemical bath deposition technique. The characterization of the nanowires was conducted using scanning electron microscopy (SEM), X-ray diffraction (XRD), energy dispersive X-ray analysis (EDX), and a spectrophotometer. The SEM images revealed that the diameters of the ZnO nanowires varied from 170.3 to 481 nm, indicating that a bath solution pH of 8.1 is optimal for the formation of hexagonal ZnO nanowires. The XRD patterns validated that the ZnO nanowires exhibit a hexagonal crystallite structure, with the crystallite size, determined via Scherrer's equation, increasing with elevated annealing temperatures (0.536 nm, 0.541 nm, and 0.557 nm at 100°C, 150°C, and 200°C, respectively). EDX analysis yielded insights into the elemental composition of the samples, confirming the presence of Zn and O. Results from optical analysis demonstrated that ZnO nanowires possess high absorbance in the ultraviolet and infrared spectra while exhibiting significant transmittance in the visible spectrum. Furthermore, the absorbance of the nanowires was found to increase with higher annealing temperatures. Their notable absorbance in the ultraviolet range indicates potential applications as solar harvesters for capturing solar energy for photovoltaic panels, which can convert sunlight directly into electricity for commercial or industrial use.

Keywords – Nanowire, ZnO, synthesis, characterization, predict application.

I. INTRODUCTION

A nanomaterial is characterized as a material made up of nanostructures that range from 1 to 100 nanometers (or billionths of a meter) in size (Obruche et al., 2018). These nanostructures may encompass nanoparticles, nanotubes (such as carbon nanotubes), nanowires, nanoporous materials, nanocomposites, or nanocrystals. (Ekpo et al., 2023). Due to the diminutive dimensions of their constituent structures, nanomaterials display characteristics that are distinctfrom those of traditional materials. A nanowire is defined as a minuscule structure with a diameter approximately equal to a nanometer (10−9 meters). Alternatively, nanowires can be characterized as structures with a thickness or diameter restricted to tens of nanometers or less, while their length can extend significantly.

At these minuscule dimensions, quantum mechanical phenomena become prominent, giving rise to the designation "quantum wires." Various types of nanowires exist, including metallic varieties (such as Ni, Pt, Au), semiconducting types (like Si, InP, GaN, ZnO, etc.), and insulating forms (for instance, SiO2, TiO2). Typical nanowires exhibit length-to-width ratios of 1000 or more, which is why they are frequently referred to as one-dimensional (1-D) materials. Nanowires possess numerous unique attributes that are absent in bulk or three-dimensional materials (Morsy et al., 2022). This distinctiveness arises from the lateral confinement of electrons in nanowires due to quantum mechanics, causing them to occupy energy levels that diverge from the continuous energy levels or bands observed in bulk materials (Itodo et al., 2021). The unique features of quantum confinement in certain nanowires lead to specific values of electrical conductance (Obruche et al., 2019). These specific values result from a quantum mechanical restriction on the number of electrons capable of traversing the wire at the nanometer scale (Amjad et al., 2019). Furthermore, nanowires demonstrate other atypical electrical properties attributable to their small size (Rabiee et al., 2022).

In contrast to carbon nanotubes, where electron movement can be described by ballistic transport (permitting electrons to traverse freely between electrodes), the conductivity of nanowires is significantly influenced by edge effects. Edge

effects emerge from atoms on the surface of the nanowire that are not completely bonded to their neighboring atoms, in contrast to those within the bulk of the nanowire (Gao et al., 2016). The presence of unbonded atoms can introduce defects within the nanowire, which may result in diminished electrical conductivity when compared to the bulk material (Obruche et al., 2018). As the size of a nanowire decreases, the proportion of surface atoms relative to those within the nanowire increases, thereby amplifying the significance of edge effects (Ogwuche & Obruche, 2020).

Furthermore, conductivity may undergo energy quantization, indicating that the energy levels of electrons traversing a nanowire can only assume specific values, which are multiples of the Von Klitzing constant (G) = 2e2/h (where e denotes the electron charge and h represents Planck's constant). Consequently, conductivity is defined as the cumulative transport through various channels characterized by distinct quantized energy levels (Peng et al., 2017). A thinner wire results in a reduced number of channels available for electron transport. The phenomenon of quantized conductivity is more pronounced in semiconductors such as Si or GaAs in comparison to metals, attributable to their lower electron density and effective mass (Ghazal et al., 2023). Evidence of quantized conductance can be observed in silicon fins measuring 25 nm in width, which leads to an increased threshold voltage (Obruche et al., 2019).

Numerous chemical, physical, and electrochemical deposition techniques have been reported for the fabrication of oriented MOS (metal oxide semiconductor) nanowires. Methods such as catalytic growth via the vapour-liquid-solid epitaxial (VSLE) mechanism, metal-organic chemical vapour deposition (MOCVD), pulsed laser deposition (PLD), chemical vapour deposition (CVD), hydrothermal synthesis, solution-based methods, and electrodeposition have proven particularly effective in producing well-aligned arrays of anisotropic ZnO nanowires (Liu et al., 2022). In general, there exist two fundamentally distinct strategies for the synthesis of nanowires: top-down and bottom-up approaches (Wang & Hu, 2014). The top-down approach typically entails etching and lithography on bulk materials to fabricate functional devices, and it has demonstrated success across various applications.

Techniques have been developed to produce nanowires through both top-down and bottom-up methods in significant quantities, utilizing processes such as arc discharge, laser ablation, and chemical vapor deposition (CVD). Most of these techniques are conducted in a vacuum or with specific process gases. The growth of carbon nanotubes (CNTs) via CVD can occur either in a vacuum or under atmospheric pressure (Obruche et al., 2022). These methods enable the production of substantial quantities of nanotubes; advancements in catalysis and continuous growth techniques are enhancing the commercial viability of CNTs. Nanowire sensors have demonstrated the capability to detect a variety of gases, including oxygen, hydrogen, NO2, and ammonia, even at minimal concentrations (Festus-Amadi et al., 2021). Furthermore, nanowires have been employed to sense ultraviolet light, monitor pH variations, and identify low-density lipoprotein cholesterol.

In the medical domain, nanowires are utilized to develop nanoscale sensors for diverse applications, such as the detection of potential cancer biomarkers (Obruche et al., 2025). For example, nano-sized sensing wires positioned across a microfluidic channel can capture molecular signatures of particles and relay the information instantaneously. These sensors are capable of identifying altered genes associated with cancer and may ultimately reveal the locations of malignant genes. In the realm of electronics, various semiconductor devices, including junction diodes, memory cells, switches, transistors, FETs, LEDs, and inverters, have been fabricated using nanowire junctions (Ekpo et al., 2024). The extensive surface area and high conductivity of nanowires render them suitable for inorganic-organic solar cells.

Research suggests that a significant number of individuals predominantly depend on non-renewable energy sources, such as coal, fossil fuels, and natural gas, as their primary energy supply (Novoselov et al., 2004). Nevertheless, the energy generated from these sources is limited, and their byproducts are not environmentally friendly, costly, and restricted in availability. Given that nature does not replenish these resources at the same pace they are utilized, they will ultimately deplete. Consequently, it is essential to pursue a more plentiful, eco-friendly, clean, affordable, and sustainable energy alternative. In this context, the optical characteristics of ZnO nanowires are being investigated to evaluate their potential as solar energy harvesters for renewable energy in industrial and commercial settings (Obruche et al., 2019).
This study aims to synthesize and characterize ZnO nanowires and utilize the results to forecast its applications.

II. MATERIALS AND METHOD

Materials

All chemicals utilized in this study were of reagent grade and did not require any further processing. All aqueous solutions were prepared using distilled water. Bendosen Zinc nitrate hexahydrate (99.9% purity), Zinc acetate dihydrate (98% purity), Ethanol (98% purity, $\rho = 0.788$ gcm-3), Ammonia (98% purity, $\rho = 0.9$ gcm-3), and Distilled water were supplied by Merck.

Substrate Preparation

Prior to the deposition of ZnO nanowires, glass micro slides were chemically degreased with dilute HCl for 24 hours, subsequently cleaned with detergent and cold water, rinsed with

distilled water, and allowed to air dry (WHO, 2010; Obruche et al., 2019).

Substrate Pretreatment

Equal volumes (10 mL) of zinc acetate dihydrate [Zn(OOCCH3)2.2H2O] (0.05M) and ethanol (0.05M) were mixed in a 50 ml beaker. This solution was applied to glass substrates using a spin coater (Laurell WS-400-STFW-FULL) at a speed of 2000 rpm for 30 seconds. The thickness of the zinc acetate layer can be modified by varying the number of spin coating cycles, demonstrating good reproducibility. In this instance, the substrates underwent spin coating on two occasions. Following this, the coated substrates were allowed to dry at ambient temperature and subsequently annealed at 150°C for a duration of 30 minutes. Prior to the final growth of ZnO nanowire, all substrates received a pretreatment twice.

Chemical Bath Deposition (CBD) Growth

To initiate the CBD growth process, an aqueous solution comprising zinc nitrate hexahydrate and hexamine was first prepared in accordance with the methodology outlined by (WHO, 2010; Obruche et al., 2018). Both substances were utilized at a concentration of 0.1M. A mixture of 20 mL of aqueous zinc nitrate hexahydrate and 20 mL of hexamine was combined in a 50 mL beaker. Aqueous ammonia (0.1M) was introduced to modify the pH level, with the quantity added determined by the target pH. In this investigation, 4-6 mL of aqueous ammonia was employed to elevate the pH to values of 9.00 and 10.0. The initial growth solution exhibited a pH of 8.1. This initial solution (pH 8.1) was transparent and contained white dispersed Zn(OH)2 precipitates.

The bath solutions at pH levels of 9.0 and 10.0 were fully dissolved and appeared milky. The pretreated glass slides (substrates) were positioned within the three distinct bath solutions, tilted against the wall of the beaker. The beakers containing the bath solutions and substrates were subjected to heating in an oven for 2 hours at a consistent temperature of 93°C. Upon completion of the growth phase, the substrates were removed from the solutions, rinsed with distilled water, and dried at room temperature. A white, dense, and uniform layer was observed on the samples cultivated at pH 8.1. Conversely, a less dense milky layer was detected on the samples at pH 9.0, while a slightly transparent white layer was noted on those at pH 10.0.

Post Growth Annealing

A thermal annealing procedure was performed on the substrates (samples) derived from the three distinct pH solutions (8.1, 9.0, and 10.0) at temperatures of 100°C, 150°C, and 200°C for a duration of 1 hour, followed by a quenching process to room temperature by removing them from the oven as described by (WHO, 2010, Obruche 2019)

Table1. Sample Identification

SAMPLE	GROWTH pH	ANNEALING °C
W8100	8.1	100
W8150	8.1	150
W8200	8.1	200
W9100	9.0	100
W9150	9.0	150
W9200	9.0	200
W10100	10.0	100
W10150	10.0	150
W10200	10.0	200

III. RESULTS AND DISCUSSION

Any synthesis process must commence with a comprehensive understanding of the composition or structure of the intended final product. A variety of techniques can be employed for this purpose, including structural analysis to evaluate the concentration and purity of the synthesized materials. To ascertain whether nanowire was produced via this method, the synthesized nanowire was subjected to analysis through SEM, EDX, and XRD. These techniques yield critical insights into the chemistry of the synthesized nanowire.

Scanning Electron Microscopy (SEM)

The results of the morphological analysis (surface structure) of the deposited ZnO nanowire were acquired using a scanning electron microscope, as depicted in Figure1, at varying pH levels. The nanowires cultivated at the standard pH of the bath solution (8.1) display a hexagonal morphology, and their diameters were measured at different angles, including 90° and 132.30°, across the width of the nanowire between two points (Pa1 & PaR1). The measurements varied from 170.3 to 481 nm, as illustrated in Figure1.

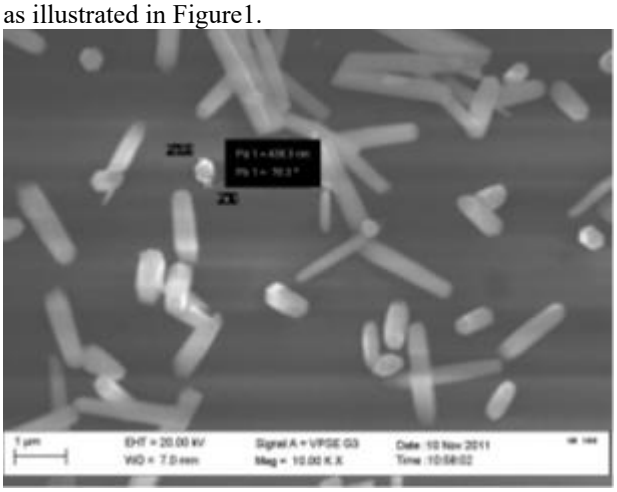

Figure.1. SEM of W8100, W8150, W8200 grown at pH 8.1 and annealed at 100 oC, 150 oC& 200°C

The specimens cultivated at pH values of 9.0 and 10.0 exhibited nanostructures that resemble tapered floral shapes, as depicted in Figures 2&3. This alteration in morphology may be attributed to the interplay between growth and erosion processes. It is widely recognized that the hexagonal wurtzite structure of ZnO is a quintessential polar crystal characterized by a dipole moment oriented along the c-axis. Consequently, the (0001) crystal plane signifies polarity and is metastable, whereas the lateral planes are non-polar and exhibit greater stability. The polar top planes have the capacity to attract OH- ions, which may lead to the erosion of these planes in the solution, as represented in the following equation:

$$ZnO + OH^- \rightarrow ZnO_2^{2-} + H_2O \quad \ldots\ldots 1$$

In the initial growth solution, the concentration of OH- present is adequate solely for the formation of the nanowires. Upon the addition of aqueous ammonia, an increased generation of OH- ions occurs when the solution is heated, ensuring that not all OH- is utilized during the growth phase.

As a result, the residual OH- in the solution also engages in the erosion reaction concurrently. The intensity of the erosion process escalates with rising pH levels. Nevertheless, during the Chemical Bath Deposition (CBD) growth process, the rate of growth exceeds that of erosion. Therefore, due to the competition between these two processes, the tips of the ZnO nanowires become tapered at pH levels ranging from 9.0 to 10.0.

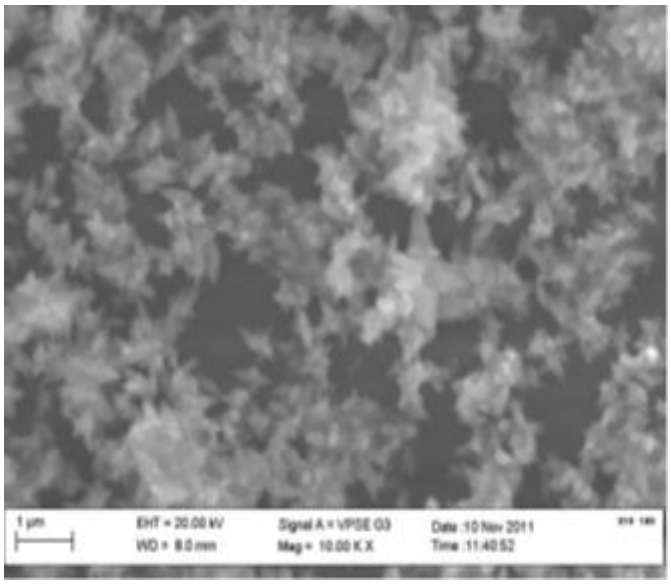

Figure 2. SEM of W9100, W9150, W9200 grown at pH 9.0 and annealed at 100 oC, 150 oC &200 oC

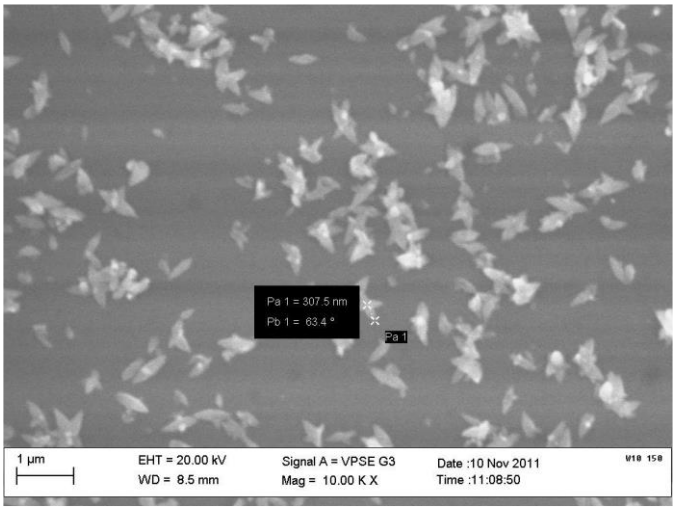

Figure 3. SEM of W10150, W10200 grown at pH 10.0 and annealed at150 oC & 200°C.

The SEM images reveal that as the growth pH rises from the initial pH of the solution, the morphology of the nanowire evolves from a hexagonal configuration to a tapered, flower-like shape. Consequently, the initial pH of 8.1 in the solution is identified as the optimal condition for the synthesis of ZnO nanowires exhibiting a hexagonal top surface.

X-Ray Diffraction (XRD)

The XRD analysis was conducted on samples developed at a pH of 8.1. To assess the crystalline characteristics of the deposited nanowires, the XRD patterns were recorded within the 2θ range of 10 - 70° utilizing CuK2 (λ = 1.5406 Å), and the intensity was plotted against 2θ. The XRD diffraction pattern along with peak values for the annealed nanowires is illustrated in Fig. 10. By correlating the angular diffraction within the 2θ range with the ZnO compound phase (Fig. 11), three peaks at 2θ values of 33.77, 44.82, and 53.63 for sample W8100 were identified, two peaks at 2θ values of 44.88 and 66.40 for sample W8150 were recognized, and three peaks at 2θ values of 31.82, 56.68, and 67.96 were identified for sample W8200.

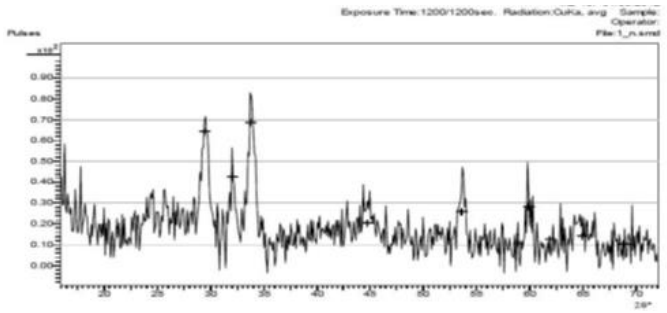

Figure 4. X-Ray Diffraction pattern of W8100, W8150 & W8200

The average crystallite sizes within the nanowires were determined utilizing the inverse relationship of the full width at half maximum (FWHM), as articulated by Debye-Scherrer's equation:

D = 0.9 λ/βcosθ ……..….2

In this equation, D denotes the crystalline size, λ signifies the X-ray wavelength employed (1.5406 A), β represents the FWHM intensity, and θ indicates the Bragg's angle (the angle of diffraction). For W8100, the three peaks at specific 2θ values corresponding to their FWHM are 33.77, 44.82, and 53.63 at 0.28912, 0.27997, and 0.27168 respectively. At θ = 33.77.

The average crystallite sizes for W8150 and W8200 were computed in a similar manner, and the findings are displayed in Table 2.

Table 2. Nanowire crystallite size

Sample	Annealing temperature (0C)	Average crystallite size (nm)
W8100	100	0.536
W8150	150	0.541
W8200	200	0.557

The information presented in the table demonstrates that the average size of the crystallites increases with the rise in annealing temperature. The X-Ray Diffraction analysis indicates that the ZnO nanowire exhibits a hexagonal crystallite structure characterized by lattice parameters: a = 0.3296, b = 0.3296, and c = 0.52065 (noting that a = b ≠ c), as depicted in Figure 10 above, which conforms to the specifications of a hexagonal lattice structure. The interplanar spacing (d), defined as the distance between lattice structures on a given plane, was determined for the sample cultivated at pH 8.1 through the application of Bragg's law for validation.

d = ……3

where, d = interplanar spacing, n = 1 for a simple lattice structure, = X-ray wavelength utilized (1.5406 A), θ = Bragg's angle (the angle of diffraction).

Table 3. Nanowire interplanar spacing

Bragg's angle(θ)	d- observed	d-calculated
16.89	2.653	2.652
22.41	2.022	2.020
26.82	1.708	1.707

The interplanar spacing (d-observed) referenced in the preceding table pertains to the measurements recorded by the diffractometer, whereas d-calculated denotes the spacing derived for the purpose of validation. The information presented in the table suggests that there is no significant disparity between d-observed and d-calculated.

UV-visible spectrophotometry

The optical properties of ZnO nanowires, cultivated at pH values of 8.1 and 9.0, were examined utilizing the (UNICO-UV-Vis-NIR 2120 PC) spectrophotometer across a wavelength range of 172.8-1100 nm. The absorbance versus wavelength graph, depicted in Figure 5&6, demonstrates that ZnO nanowires display considerable absorbance within the ultraviolet spectrum (175.85nm).

However, the absorbance progressively diminishes in the visible spectrum while increasing towards the infrared region. Conversely, transmittance, T, experiences a decline as absorbance escalates.

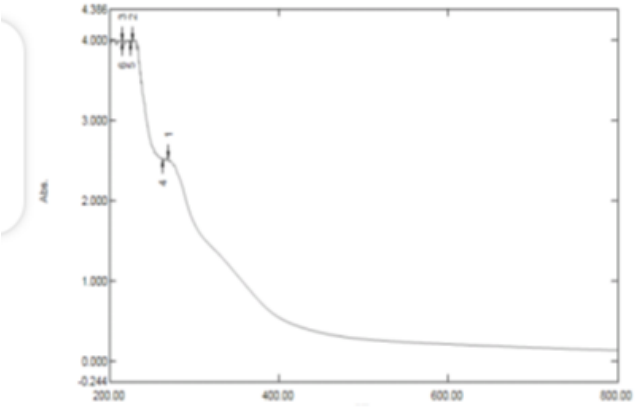

Figure 5. Uv absorbance vs wavelength for W8100,W8150 & W8200.

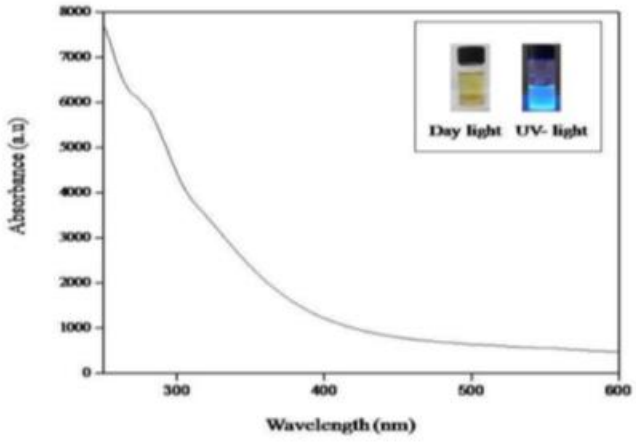

Figure 6. A graph illustrating the relationship between absorbance and wavelength for W9100, W9150, and W9200.

The correlation graphs depicting absorbance against wavelength in Figures 12 and 13 demonstrate a consistent increase in absorbance with rising annealing temperatures. At a pH level of 8.1, the absorbance measurements recorded were 0.82, 0.84, and 0.85 at temperatures of 100°C, 150°C, and 200°C, respectively. Conversely, at a pH of 9.0, the absorbance values were 0.46, 0.64, and 0.71 at the same temperature points. The elevated absorbance observed in the ultraviolet spectrum indicates its potential application as a solar harvester, capable of capturing solar energy for photovoltaic panels, which can directly convert sunlight into electricity for commercial or industrial use.

Energy Dispersive X-ray Analysis (EDX)

The compositional analysis of the deposited ZnO nanowire was conducted using energy dispersive X-ray (EDX) at a voltage of 14KV. The resulting spectra reveal peaks that encompass both the elemental compositions of the glass substrate and the deposited nanowire. Each element possesses a unique atomic structure and binding energy. When in a stable state, an atom within the sample contains ground state (or unexcited) electrons situated in specific energy levels or electron shells that are bound to the nucleus.

The incoming beam excites an electron from an inner shell, resulting in its ejection and the formation of an electron hole. An electron from an outer, higher energy shell subsequently fills this hole, and the energy difference between the two shells is emitted as an X-ray. The quantity and energy of the X-rays released from a specimen are characteristic of a specific element, leading to distinct sets of peaks in its X-ray spectrum. The spectra were consistent across all samples. Figure 7 present the EDX results for samples W8100 and W9100.

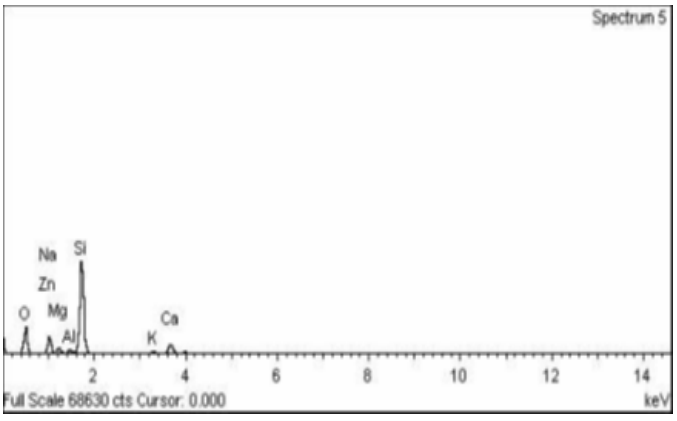

Figure 7. EDX spectrum of W8100, W9100 grown at pH of 8.1 & 9.0

The weight composition of the elements found in both the nanowire and the glass substrate is presented in Table 4.

Table 4. Elemental composition

Element	Weight (%)
Oxygen (O)	36.28
Aluminum (Al)	0.72
Silicon (Si)	26.59
Potassium (K)	0.55
Calcium (Ca)	3.50
Zinc (Zn)	29.16
Sodium (Na)	1.06
Magnesium (Mg)	2.14

The elemental composition presented in the table above validated the presence of Zinc (29.16%) and Oxygen (36.28%), which are integral components of Zinc oxide nanowire.

IV. CONCLUSION

This study illustrated that a well-aligned ZnO nanowire can be synthesized through the chemical bath deposition technique, with a bath solution pH of 8.1 identified as the optimal condition for producing ZnO nanowires featuring a hexagonal top surface. Furthermore, this research revealed that both the crystallite size and the absorbance of the nanowire increase with rising annealing temperatures. Its notable absorbance in the ultraviolet spectrum indicates its potential application as a solar harvester for capturing solar energy for photovoltaic panels, which can directly convert sunlight into electricity for commercial or industrial use.

REFERENCES

1. Amjad, M., Iqbal, M., Faisal, A., Junjua, A. M., Hussain, I., Hussain, S. Z., Ghramh, H. A., Khan, K. A., & Janjua, H. A. (2019). Hydrothermal synthesis of carbon nanodots from bovine gelatin and PHM3 microalgae strain for anticancer and bioimaging applications. Nanoscale Advances, 1(8), 2924–2936.
2. C. Liu, H. Li, R. Cheng, J. Guo, G.-X. Li, Q. Li, C.-F. Wang, X. Yang, S. Chen, (2022). Facile synthesis, high fluorescence and flame retardancy of carbon dots, Journal of Materials Science & Technology 104,163-171.
3. Ekpo Rose, Obruche E.K, and Marcus. A. (2024). Spatial and Temporal Variations in the Concentrations of Polycyclic Aromatic Hydrocarbon, in Ambient Air From Three Different Locations in River State, Nigeria. International Journal of New Chemistry, 12 (4), 567-580

4. Festus-Amadi, I. R, Erhabor, O. D, Ogwuche Christiana E, and Obruche E. K. (2021). Characterization of Contaminated Sediments Containing Polycyclic Hydrocarbons from Three Rivers in the Niger Delta Region of Nigeria. Chemistry Research Journal, 6(3):1-12
5. Gao, X., Du, C., Zhuang, Z., & Chen, W. (2016). Carbon quantum dot-based nanoprobes for metal ion detection. Journal of Materials Chemistry C, 4(29), 6927-6945.
6. Ghazal, S. Shaker, E. Abdelaziz, (2023). Synthesis of carbon dots and its applications in textiles, Egy. J. Chem. 66(12),71-86.
7. Itodo, A. U., Wuana, R. A. Erhabor, O. D., Obruche, E. K. and Agbendeh, Z. M.(2021). Evaluating the Effects of Roofing Materials on Physicochemical Properties of Harvested Rainwater in Warri, Delta State, Nigeria. Chemical Society of Nigeria Journal, Kano, 12(1): 234-245
8. M. Morsy, A. Elzwawy, M. Oraby, (2022).Carbon nano based materials and their composites for gas sensing applications: Review %j egyptian journal of chemistry, 65(5),691-714.
9. Novoselov, K. S., Geim, A. K., Morozov, S. V., Jiang, D. E., Zhang, Y., Dubonos, S. V., ... & Firsov, A. A. (2004). Electric field effect in atomically thin carbon films. science, 306(5696), 666-669.
10. Obruche E. k, Erhabor O.D, Itodo A.U and Itopa S.T (2019). Spectrophotometric determination of iron in some commercial iron containinig tablets/capsule. International journal of advanced trends in computer applications, 1(1): 231-235
11. Obruche E. K, Ogwuche C.E, Erhabor O.D and Mkurzurum.C (2018). Evaluation of the inhibitive effect of African Marigold (Tagetes erectal L.) Flower Extracts on the Corrosion of Aluminium in Hydrochloric Acid. International Journal of Advances in Scientific Research and Engineering, 4 (12): 167-177
12. Obruche E. K, Ogwuche C.E, Erhabor O.D and Mkurzurum.C (2019).Investigating Corrosion Inhibition Effects of Tagetes Erecta L. Leaf Extrac on Aluminium in Acidic Medium. Global Scientific Journals, 7 (1): 1-17
13. Obruche E. K, S.O Emakunu, & G.C Ugochukwu (2025). Rainwater harvesting:microbial asnd chemical water quality assessment in warri district. Mosogar journal of science education, 10(1): 36-46
14. Obruche E.K, Itodo Adams, Wuana Raymond and Sesugh Ande (2022). Polycyclic Aromatic Hydrocarbons in Harvested Rainwater in Warri and Agbarho, Nigeria. Bulletin of chemical society of Ethiopia, 36(4): 27-35
15. Ogwuche C.E and Obruche E.K. (2020). Physio-chemical analysis of palm oils (elaeis guineensis) obtained from major markets in agbarho, unenurhie, opete, ughelli and evwreni town, Delta state, Nigeria. International journal of trend in scientific research and development,4(2):56-60
16. Peng, Z., Miyanji, E. H., Zhou, Y., Pardo, J., Hettiarachchi, S. D., Li, S., ... & Leblanc, R. M. (2017). Carbon dots: promising biomaterials for bone-specific imaging and drug delivery. Nanoscale, 9(44), 17533-17543.
17. R.E. Ekpo, A.C. Marcus and E.K. Obruche (2023). Spartial and Temporal Variations in the Concentration of Particulate Matter in Ambient Air from three Different Locations in River State, Nigeria. International Journal of Scientific Research in Chemical Science,10(4):32-38
18. Rabiee, N., Iravani, S., & Varma, R. S. (2022). Biowaste-derived carbon dots: a perspective on biomedical potentials. Molecules, 27(19), 6186.
19. Wang, Y., & Hu, A. (2014). Carbon quantum dots: synthesis, properties and applications. Journal of Materials Chemistry C, 2(34), 6921 6939.
20. WHO (2010).Guidelines for Safe drinkable Water, Fresh waters and waste water. Retrieved from www.who.org/media/media_27228.,(accessed 21/1/2019).